0888-8809/05/$15.00/0
Printed in U.S.A.

Molecular Endocrinology 19(6):1569–1583

doi: 10.1210/me.2004-0528

p38 Mitogen-Activated Protein Kinase (MAPK) Is a Key Mediator in Glucocorticoid-Induced Apoptosis of Lymphoid Cells: Correlation between p38 MAPK Activation and Site-Specific Phosphorylation of the Human Glucocorticoid Receptor at Serine 211

Aaron L. Miller, M. Scott Webb, Alicja J. Copik, Yongxin Wang, Betty H. Johnson, Raj Kumar, and E. Brad Thompson

Department of Human Biological Chemistry and Genetics, University of Texas Medical Branch, Galveston, Texas 77555-1068

Glucocorticoids (GCs) induce apoptosis in lymphoid cells through activation of the GC receptor (GR). We have evaluated the role of p38, a MAPK, in lymphoid cell apoptosis upon treatment with the synthetic GCs dexamethasone (Dex) or deacylcortivazol (DAC). The highly conserved phosphoprotein p38 MAPK is activated by specific phosphorylation of its threonine180 and tyrosine182 residues. We show that Dex and DAC stimulate p38 MAPK phosphorylation and increase the mRNA of MAPK kinase 3, a specific immediate upstream activator of p38 MAPK. Enzymatic assays confirmed elevated activity of p38 MAPK. Pharmacological inhibition of p38 MAPK activity was protective against GC-driven apoptosis in human and mouse lymphoid cells. In contrast, inhibition of the MAPKs, ERK and cJun N-terminal kinase, enhanced apoptosis. Activated p38 MAPK phosphorylates specific downstream targets. Because phosphorylation of the GR is affected by MAPKs, we examined its phosphorylation state in our system. We found serine 211 of the human GR to be a substrate for p38 MAPK both *in vitro* and intracellularly. Mutation of this site to alanine greatly diminished GR-driven gene transcription and apoptosis. Our results clearly demonstrate a role for p38 MAPK signaling in the pathway of GC-induced apoptosis of lymphoid cells. (*Molecular Endocrinology* 19: 1569–1583, 2005)

THE MECHANISM by which glucocorticoids (GCs) bring about the apoptotic death of lymphoid cells is not clear. However, some important landmarks in the process have been identified (1–3). It has been established that an interval of continual steroid exposure is required, up to many hours in malignant lymphoid cells. Sufficient levels of active intracellular GC receptor (GR) are necessary during this time, and the steroid-activated GR evokes a network of regulatory events. Eventually, more and more cells become inextricably committed to overt apoptosis. When it was first recognized that the cell death evoked by activated GR was apoptotic, it was hoped that this might simplify the problem, but this expectation has waned as awareness of the complexity of mammalian apoptotic pathways has increased (4–8). It is certain now that the antecedent gene network affected by GCs involves a dense amount of signal pathway cross talk (1–3). Consequently, considerable effort has been devoted to the identification of the critical regulated genes. Transcriptional induction or suppression of some genes has been clearly identified, and the use of gene array data has led to recognition of a number of additional candidate genes that deserve further experimental testing (9–12). The GC/GR-driven pathway to apoptosis of lymphoid cells is strongly influenced by other cellular signaling systems that function at a posttranslational level, to control the activity of enzymes and transcription factors. The cAMP/protein kinase A pathway synergizes strongly with the GC-GR system in producing lymphoid-cell apoptosis (13–15). Other evidence shows that the redox balance of the cell (16), members of the protein kinase C pathways (17–19), and other posttranslational regulatory systems (20, 21) also have potent influences. Before the work reported here, several lines of evidence hinted at the possibility that the MAPKs might also be involved.

The MAPK signaling system has been implicated in gene induction by GCs (22–25). In several cell sys-

First Published Online April 7, 2005

Abbreviations: AF, Activation function domain; DAC, deacylcortivazol; Dex, dexamethasone; DMSO, dimethylsulfoxide; ECFP, enhanced cyan fluorescent protein; EGFP, enhanced green fluorescent protein; FBS, fetal bovine serum; G, threshold cycle; GC, glucocorticoid; GR, GC receptor; GRE, GC response element; hGR, human GR; JNK, cJun N-terminal kinase; MKK3, p38-specific upstream kinase kinase; PI, propidium iodide; PVDF, polyvinylidine difluoride; S211, serine 211; SEAP, secreted placental alkaline phosphatase; TBS, Tris-buffered saline.

***Molecular Endocrinology* is published monthly by The Endocrine Society (http://www.endo-society.org), the foremost professional society serving the endocrine community.**

tems, MAPKs have been found to play a role in apoptosis initiated by mechanisms other than GCs (26–33). We therefore tested the contributions of three major MAPKs in the apoptosis specifically evoked by GCs in malignant lymphoid cells. We show that p38 MAPK is a component of the GC-evoked pathway to lymphoid cell apoptosis in human and mouse cell systems and that the p38-specific upstream kinase kinase MKK3 appears to be involved. In contrast to p38, other major MAPKs, *viz.* ERK and cJun N-terminal kinase (JNK), appear to support cell viability in the context of GCs. We further find that site-specific phosphorylation of the human GR (hGR) N-terminal activation function domain (AF1) by p38 MAPK is involved in the apoptotic and gene-inductive events initiated by GC.

RESULTS

Specific Inhibition of MAPKs in Human and Mouse Cells Reveals that p38 MAPK Activity Is an Important Component in GR-Dependent Lymphoid Cell Apoptosis

To test the relevance of p38 MAPK activity, several clones of CEM (human) cells and the S49.1 clone of mouse cells were examined. Two highly specific inhibitors of p38 MAPK were employed. The use of two inhibitors helped rule out nonspecific effects due to a particular chemical structure. ICR-27 cells (34) are a subclone of CEM cells selected after mutagenesis from the GC-sensitive clone CEM-C7, for resistance to apoptosis in high concentrations of the synthetic GC dexamethasone (Dex). The basis for this insensitivity is lack of functional GR because the sensitivity of ICR-27 cells to Dex-evoked apoptosis is restored after supplying them with GR via transfection (35). We repeated and confirmed that experiment by transfecting the cells with plasmids expressing an enhanced green fluorescent protein (EGFP) fused to the hGR. When subsequently treated with Dex, significant apoptosis ensued in those cells that had received the EGFP:hGR gene. This apoptotic effect was completely prevented by simultaneous addition of equimolar RU486, a competitive antagonist for the GR (data not shown). Thus, the apoptotic response was entirely dependent on the steroidal activation of the transfected GR. When SB203580, a specific blocker of the p38 MAPK, was added along with Dex, the steroid-induced apoptosis was prevented for at least several days (Fig. 1).

This dependence of GR-evoked apoptosis on p38 MAPK activity is not limited to one particular clone of human cells. S49 cells are mouse lymphoid cells, perhaps the first lymphoid line shown to be susceptible to GC-evoked apoptosis (36). As with ICR-27 cells that had been restored to Dex sensitivity by provision of adequate GR, inhibition of p38 MAPK in the naturally sensitive S49.1 clone blocked the cells' apoptotic response to Dex. A demonstration of this is shown in Fig. 2, depicting an experiment measuring the subdiploid

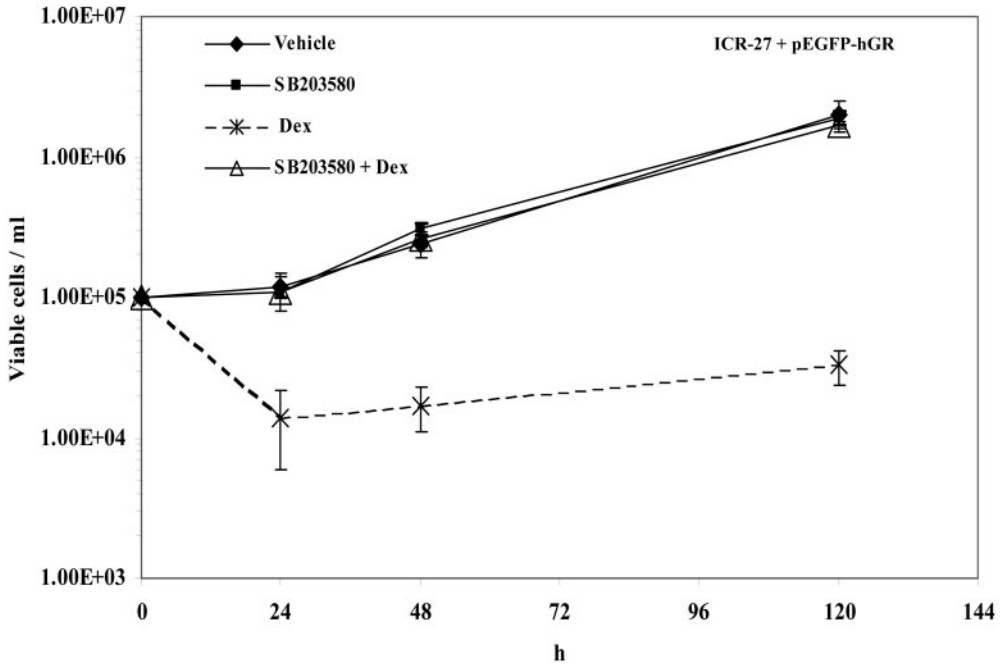

Fig. 1. p38 MAPK Activity Is Necessary for GC-Evoked Apoptosis of ICR-27 Cells Transfected with hGR

ICR-27 cells were transfected at greater than 90% efficiency with an expression vector bearing the hGR gene fused with EGFP. Twenty-four hours later, the cells were plated at 1.0×10^5 viable cells/ml and treated with vehicle (ethanol/DMSO) only (♦), 10^{-6} M Dex (*), 1.0 μg/ml SB203580, a specific inhibitor of p38 MAPK activity (■), or both together (△). Viable cells were counted thereafter for 5 d. *Error bars*: 1 SD; n = 3. One of two experiments with comparable results.

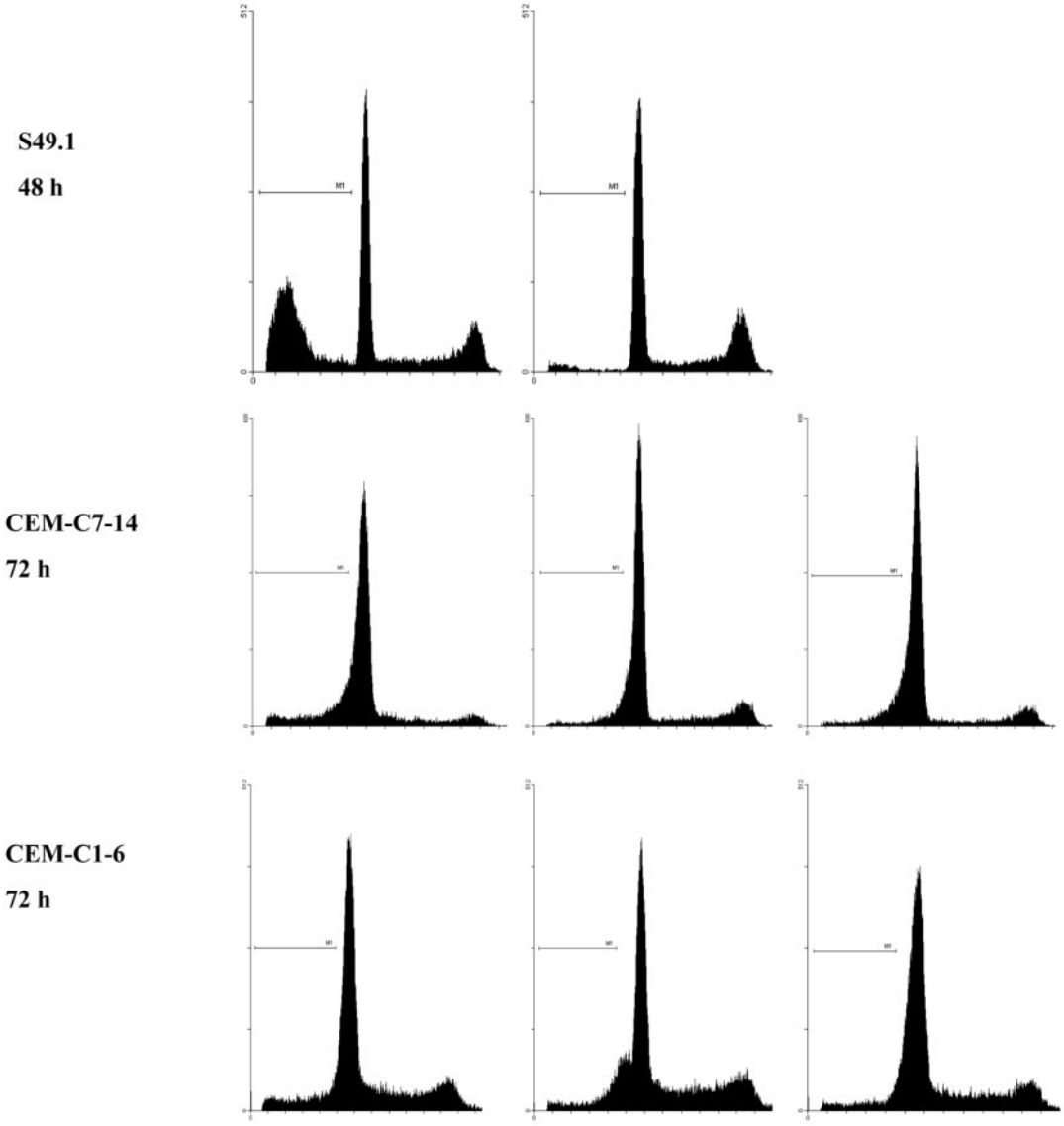

% Sub-diploid	Vehicle	Dex	Dex + SB202190	Dex + SB203580
S49.1	0.59	39	5	*
CEM-C7-14	0.54	19	9	14
CEM-C1-6	1.9	13	9	8

Fig. 2. Inhibiting p38 MAPK Activity Reduces GR-Dependent Apoptotic DNA Lysis in Mouse S49.1 Lymphoma and Human CEM Lymphoid Leukemia Cells

The histograms depict propidium iodide stained cells to show cellular DNA content. M1 represents cells with a subdiploid content of DNA. Cells were exposed to 48 h (S49.1) or 72 h (CEM) of 10^{-6} M Dex alone or together with the p38 MAPK activity inhibitors SB203580 or SB202190 (1.0 μg/ml) before staining and analysis by flow cytometry. Each histogram represents results from counting 20,000 events. The *inset table* represents percentage of cells with subdiploid DNA content; *, not done. n = 1 experiment with S49.1 cells; one of two experiments with CEM-C7–14 and CEM-C1–6 cells shown. Two additional experiments confirmed protection of S49.1 cells' viability when p38 was blocked with either SB203580 or SB202190.

content of DNA in S49 cells—a classic index of apoptosis. S49.1 cells treated with Dex display marked intracellular DNA lysis as they undergo apoptosis, as the data show. Addition of either specific inhibitor of p38 MAPK activity prevented most of this apoptotic response. Data are shown for the inhibitor SB202190. Although GC-sensitive human CEM lymphoid clones do not exhibit such marked DNA lysis as S49 cells, it can be demonstrated (37), and Fig. 2 also shows data indicating that inhibiting p38 MAPK activity reduces Dex-induced intracellular DNA lysis in two clones of apoptosis-sensitive CEM cells that naturally contain functional GR. This effect correlates in these clones with considerable, although not total, protection of cell viability in the face of Dex. Figure 3 shows the results of one such experiment, done in triplicate. In four similar experiments, after 72 h of treatment, there was an average increase of 2.3-fold in viable cells when one of the specific p38 MAPK inhibitors was added along with the Dex. Similar results were obtained when the cells were treated with deacylcortivazol (DAC): inhibition of p38 with either SB compound clearly reduced apoptosis (data not shown).

We have shown that the rapid and sustained suppression of c-*myc* transcription by Dex-activated GR is an important component in the process leading to initiation of apoptosis (38–40). Transient or chronic expression of c-*myc* partially protects against Dex-initiated apoptosis (39, 41). Consequently, we tested the effect of inhibiting p38 activity coupled with sus-

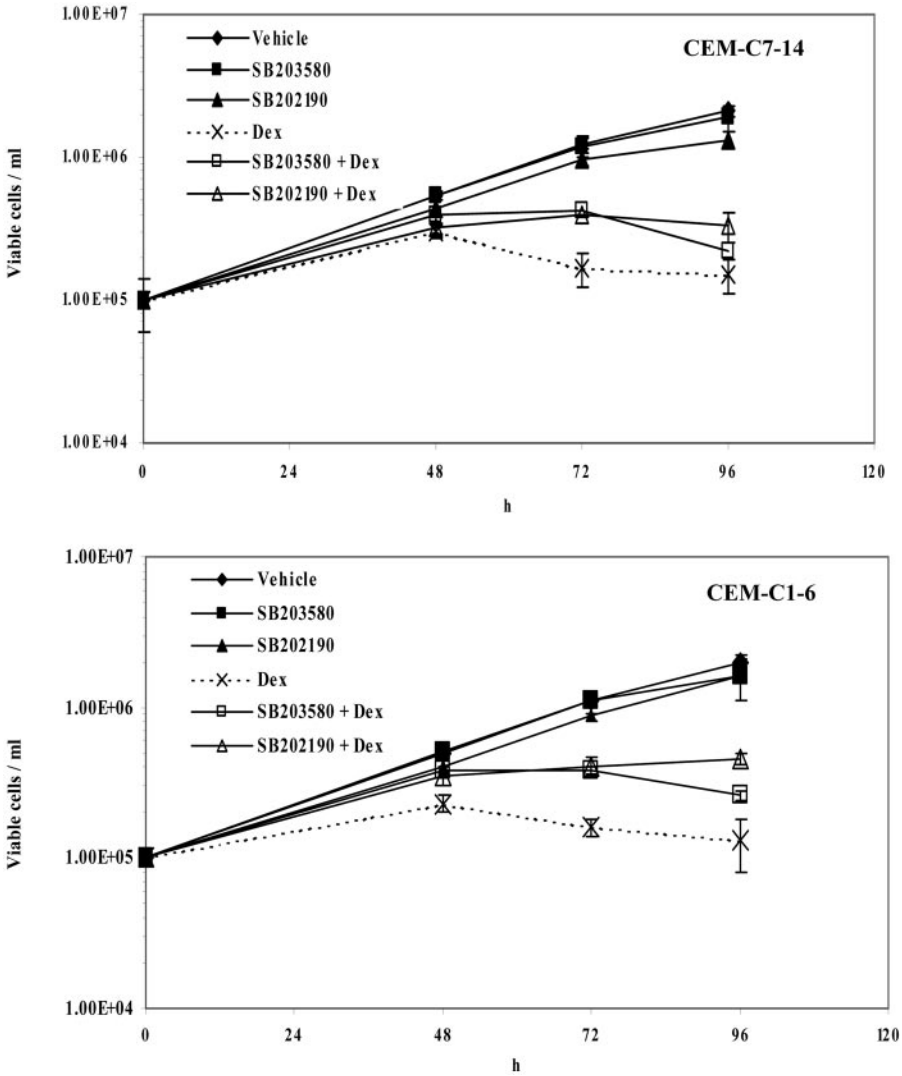

Fig. 3. Inhibition of p38 MAPK Activity Ameliorates Dex-Driven Apoptosis in Two Clones of Nonmutagenized CEM Cells

Cultures of CEM-C7–14 and CEM-C1–6 cells were exposed to vehicle (♦) (<1% ethanol), 10^{-6} M Dex (*), specific p38 MAPK activity inhibitors 1.0 μg/ml SB203580 (■) or 1.0 μg/ml SB202190 (▲), or combinations of the inhibitors plus Dex (□, △). The cultures were then followed for content of viable cells. *Upper graph*, CEM-C7–14; *lower graph*, CEM-C1–6 cells. *Error bars*: 1 SD, n = 3. One of four experiments each with triplicate biological samples of CEM-C7–14 cells is shown. Single triplicate experiment with CEM-C1–6 cells. (See also independent experiment on CEM-C1–6, Fig. 2.)

Table 1. The Proportion of Cells Surviving Dex Increases When p38 Is Inhibited in CEM-C7-14 Cells that Constitutively Express cMyc

Viable Cells per Milliliter ($\times 10^5$) after 3 d						% Survivors		
Cells: CEM-C7-14 Myc ER			Dex+		Dex+	Dex only	Dex + 203580	Dex + 202190
0 Drug (A)	SB203580 (B)	SB202190 (C)	Dex (D)	SB203580 (E)	SB202190 (F)	(D/A) × 100	(E/B) × 100	(F/C) × 100
11.5 (±3.3)	11.6 (±3.0)	8.9 (±2.5)	4.0 (±0.8)	7.5 (±0.8)	5.8 (±1.2)	35	65	65
Cells: CEM-C7-14								
10.0	9.6	8.4	1.6	4.1	3.8	16	43	45

Data from independent experiments on CEM-C7-14 and CEM-C7-14 Myc ER cells. Cells plated in equal numbers were at once treated with the agents indicated. After 3 d, viable cells were counted. Shown are averages from triplicate biological experiments for CEM-C7-14 Myc ER cells (1 SD) and the average of two experiments for CEM-C7-14, both of which show added protection with the use of the p38 activity inhibitors. *Left* (*Unshaded area*), Average viable cells from three wells. *Right* (*Shaded area*), Percentage of viable cells relative to matched control as indicated.

tained c-*myc* expression on the viability of the partially protected CEM cells treated with Dex. For this purpose, we compared effects in clone CEM-C7–14 (endogenous cMyc suppressed by Dex) and CEM-C7–14 Myc ER clone 22 (carrying a constitutive c-*myc* gene). Equal numbers of cells were plated in multiple wells of a tissue culture plate, and Dex was added to a concentration of 10^{-6} M to all but the control wells. The combination of p38 inhibitor and constitutive cMyc proved to be additive; this can be seen by comparing the percentage of cells surviving after 3 d of treatment in Dex alone with the surviving fraction treated with Dex plus inhibitors of p38 MAPK (Table 1). In the cells expressing cMyc constitutively, the fraction of survivors is greater with use of either p38 inhibitor than it is in the same CEM clone lacking constitutive cMyc. The proportionate effect of the p38 MAPK inhibitors on Dex-induced apoptosis is about the same in both clones. Blocking p38 MAPK in either CEM-C7–14 or CEM-C7–14 Myc ER cells increases surviving cells by 2- to 3-fold (compare columns D–F of Table 1). Thus, the proportional effect of the inhibitors is the same in both CEM-C7–14 cells (in which Dex blocks c-*myc* transcription and thereby lowers cMyc) and cMyc-constitutive CEM-C7–14 Myc ER cells. These results suggest that providing cMyc and blocking p38 MAPK are largely independent prosurvival events.

CEM-C7–14 Myc ER cells were also used during the experiment to examine the effect of varying the time of inhibition of p38 MAPK after addition of Dex. Each of the two specific inhibitors of p38 MAPK was added to the Dex-treated wells at three times: simultaneously with Dex, 24 or 48 h later. After 3 d total, all cells were counted. The data show that although the greatest protection is afforded when p38 is inhibited as Dex is administered, significant protection occurs upon adding the inhibitor 24 or even 48 h after the steroid (Table 2). This suggests that a phosphoprotein that must be replenished is needed for the GC-driven apoptotic process.

Table 2. Viable Cells per Milliliter ($\times 10^5$) after 3 d

Time of Addition (Days)	Vehicle	Dex	SB203580		SB202190	
			Alone	Dex (at 0) Plus SB	Alone	Dex (at 0) Plus SB
0	12.5	3.8	12.5	7.8	9.6	6.2
1				7.0		4.9
2				6.2		4.2

Effect of time of addition of p38 MAPK inhibitors on their protection against Dex-induced apoptosis of CEM-C7-14 Myc ER cells. Average of two experiments.

The important supportive role of p38 MAPK activity for GC-GR-evoked apoptosis is unique among the three major MAPKs tested. Inhibition of either ERK or JNK alone had a small effect on cell growth over several days with about a 30% reduction of cell numbers and no loss in viability. When either of these MAPKs was inhibited, however, Dex-evoked apoptosis of CEM cells was enhanced. Figure 4 shows an example of the effect of blocking JNK or ERK when Dex was supplied to the medium surrounding Dex-sensitive CEM cells. Inhibition of either MAPK significantly increased the numbers of cells killed by 10^{-6} M Dex after 72 h.

p38 MAPK Activity, Not mRNA, Is Increased by GC; Intermediate Upstream Kinase (MKK3) mRNA Is Induced

The above results raise the question of the level at which the steroid-activated GR and p38 pathways interact. We took advantage of our data from Affymetrix gene chip assays to screen for initial answers to this question. In addition to results from 20 h of exposure to Dex (9), we examined unpublished data from 2–12 h of treatment with the steroid (submitted in detail elsewhere; Webb, M.S., A. Miller, Y. Fofanov, and E. B. Thompson). No consistent evidence was found for multifold increases in p38 mRNA levels, although sporadic modest (up to 50% above controls) increases were noted (data not shown). This suggested that either constitutive levels of p38 activity

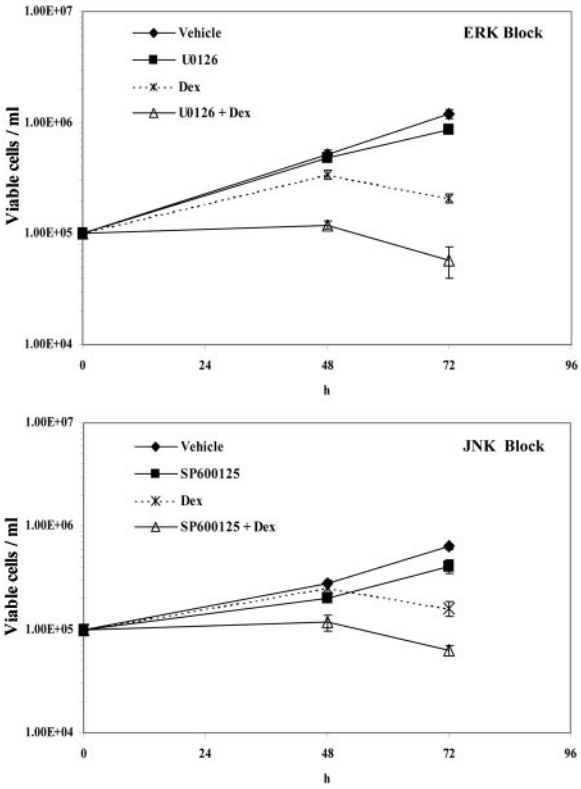

Fig. 4. Inhibition of MAPKs ERK or JNK Enhances Dex-Evoked Apoptosis of Dex-Sensitive cells, CEM Clone CEM C7–14

Cells in log growth were plated at 1.0×10^5 viable cells/ml and treated with vehicle (♦) (<1% ethanol/DMSO), 10^{-6} M Dex alone (*), ERK-inhibitor U0126 1.0 μg/ml (*upper panel*) or JNK inhibitor SP600125 1.0 μg/ml (*lower panel*) (■), or with a combination of inhibitor plus Dex (△). Viable cells counts were obtained 48 and 72 h later. *Error bars*: 1 SD; n = 3. One of two experiments with essentially the same results.

were sufficient to support Dex-induced apoptosis, or that the steroid somehow caused p38 activation. The MAPKs are activated by site-specific phosphorylations, carried out by the MAPK kinases (MAP2Ks/MKKs). For the most part, these also showed little change, with one significant exception: as judged by the gene chip array data, *mkk3*, a p38-specific immediate upstream activating kinase, was induced modestly by steroid, although not to the often-used 2-fold cutoff. To substantiate these suggestive results, we performed PCR and Northern blot analyses to evaluate MKK3 mRNA levels. Northern blots of total cellular RNA confirmed a modest, but clear increase in MKK3 mRNA levels after a 24-h exposure to either 10^{-6} M Dex or 10^{-7} M DAC, an even more potent synthetic GC (Fig. 5A). RT-PCR (not shown) and quantitative PCR (Fig. 5B) experiments further confirmed that each GC caused modest, but significant increases in MKK3 mRNA. This response is not unique to the human cell model. In mouse S49.1 cells, both steroids raised the MKK3 mRNA levels about 2-fold after an 8-h exposure, as estimated by RT-PCR (data not shown). Levels of mRNA for MKK6, the other kinase kinase specifically responsible for phosphorylation of p38, showed no regulatory response to either steroid (not shown).

We also examined the phosphorylation/activation of p38 after steroid treatment. Phosphorylation of p38 on threonine180 and tyrosine182 by MKKs activates its kinase function. By use of polyclonal antibodies specific for p38 phosphorylated at these sites, we found that both Dex and DAC brought about activation of p38 in S49.1, CEM-C7–14, and CEM-C1–6 cells (Fig. 6), whereas p38 protein levels remained nearly constant. We also noted that control levels of p38 phosphorylation varied considerably as the CEM cells were disturbed by being plated out and subsequently grown in culture without added steroids. Disturbing the cells, when setting up the experiment, raised phospho-p38 levels temporarily (2 h controls Fig. 6A), but by 8 h, the control levels had fallen considerably; thereafter, they rose slightly until 32 h, the last time sampled. At 8 h and beyond, both Dex and DAC caused an increase over controls in the site-specific, activating phosphorylation of p38 (Fig. 6B). Control mouse S49.1 cells did not show elevated phospho-p38 2 h after being replated but did show a rise in control levels thereafter. An increase in phosphorylated p38 in the Dex-treated mouse cells is clearly seen by 24 h. Activation of p38 was confirmed by direct assay of its protein kinase function in cell extracts. Figure 7 shows the results of such an assay in CEM-C1–6 extracts, demonstrating a statistically significant increase of *in vitro* p38 protein-kinase activity after 20 h of treatment of the cells with either 10^{-6} M Dex or 10^{-7} M DAC. Thus, the GCs cause a modest, but clear increase in the mRNA for MKK3, a specific activating kinase for p38, and also bring about an increase in phosphorylation/activation of p38.

Serine 211 (S211) of the Human GR Is a Site-Specific Target of Phosphorylation by p38 MAPK and Is Important in Apoptosis

These cumulative results strongly suggest that GC treatment of apoptosis-prone mouse and human lymphoid cells leads to activation of the p38 MAPK, in part at least, due to the induction of *mkk3*. The activity of the p38 kinase clearly plays an important role in the eventual death of the cells (Figs. 1–3; and Tables 1 and 2). Consequently, it may be asked, what are the protein substrates of p38 that are important in this process? Because it has been shown that GC-dependent phosphorylation at S211 of the hGR is important for the nuclear localization of the hGR (43), and because this serine lies in the important N-terminal AF1 of the hGR, we tested the possibility that the hGR S211 might be an as yet unrecognized substrate of p38. *In vitro* comparisons of several protein kinases showed that p38 was a potent kinase for S211 on the hGR. Purified recombinant AF1 domain of the hGR was incubated with several purified kinases: p38, ERK 2, Cdc 2, and casein kinase II. The reactions were eval-

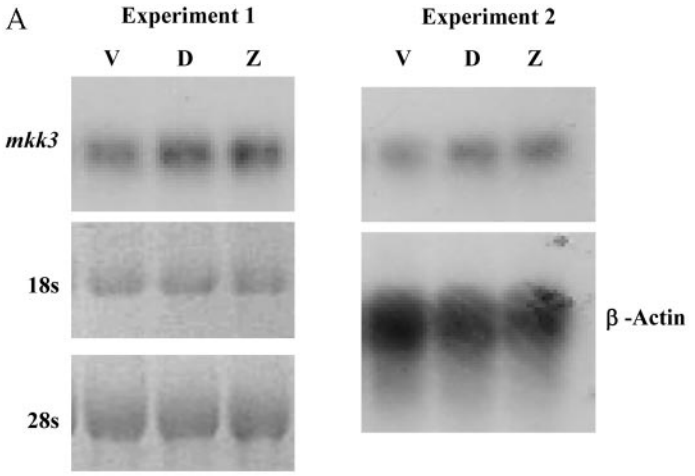

Fold Induction

	Experiment 1	Experiment 2
Dex (D)	1.45	1.4
DAC (Z)	1.9	1.9

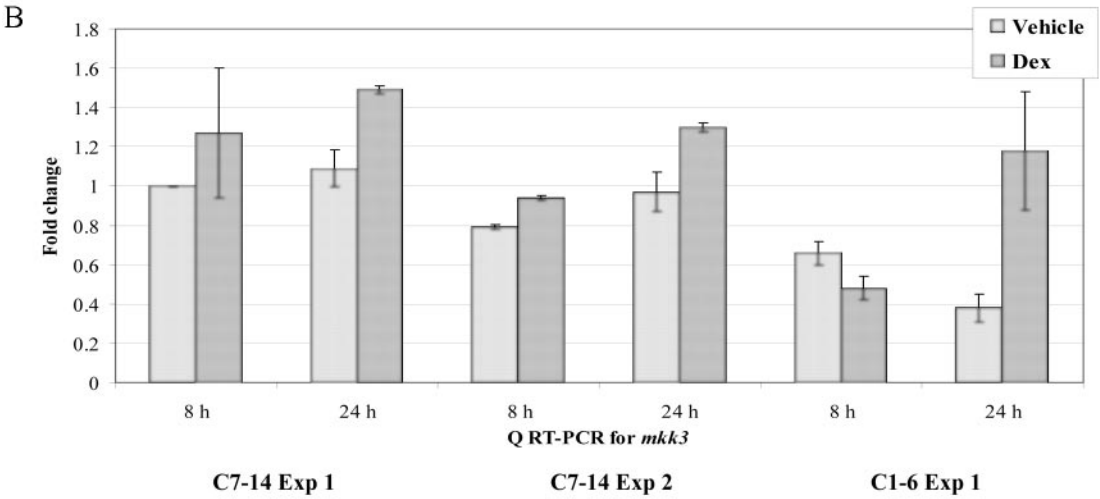

Fig. 5. GCs Cause an Increase in MKK3 mRNA in CEM-C7–14 and CEM-C1–6 Cells

CEM-C7–14 cells were grown for 24 h in medium containing vehicle (<1% ethanol/DMSO) (V), 10^{-6} M Dex (D), or 10^{-7} M DAC (Z). Cellular RNA was extracted, electrophoresed on an agarose gel, transferred to a nylon membrane, and blotted with ^{32}P labeled cDNA probe for MKK3. The blots were evaluated by densitometry and the signal intensities were normalized to either 18s RNA on the same filter (experiment 1) or to β-actin, which was detected by stripping and reprobing the same filter (experiment 2). The table shows the calculated folds of induction in response to each of the GCs (A). B, An experiment following MKK3 mRNA by quantitative PCR in CEM-C7–14 (two independent experiments) and CEM-C1–6 (one experiment) treated with vehicle (<1% ethanol) or 10^{-6} M Dex for 8 and 24 h. All data are expressed relative to the 8 h control, C7–14, experiment 1, set as 1-fold.

uated by separating the proteins with gel electrophoresis and immunoblotting with polyclonal antibodies specific for phosphorylated S211 of the hGR. Of the kinases tested, only p38 and ERK phosphorylated the site *in vitro* (Fig. 8). We then tested whether the three MAPKs contributed to AF1 S211 phosphorylation *in vivo*. Dex or DAC was added to cultures of CEM C7–14 cells, and 20 h later extracts were prepared for immunochemical analysis of the phosphorylation state of S211. Use of the two GCs serves essentially as duplicates, while ruling out a peculiar, steroid-specific effect. As others (42) have shown, corticoid treatment markedly increased S211 phosphorylation. In our hands, addition of a p38 inhibitor to the culture medium reduced this effect by about one third, whereas inhibitors of ERK or JNK did not block the phosphorylation; if anything, ERK block increased it (Fig. 9).

Because, *in vitro* and *in vivo*, p38 could act to phosphorylate the GR at this specific site, we tested whether this was relevant to GR function. It has long been known that removal of its ligand binding domain results in a constitutively active GR (43). CV-1 cells, which do not contain a functional GR, were transfected with an expression plasmid encoding hGR500, a constitutively active form of the hGR (44–46). hGR500 contains the entire N-terminal and DNA binding portions of the receptor. When bound to a GC response element (GRE) via its DNA binding domain, the powerful AF1 transactivating domain in the N-terminal portion of hGR500 causes increased tran-

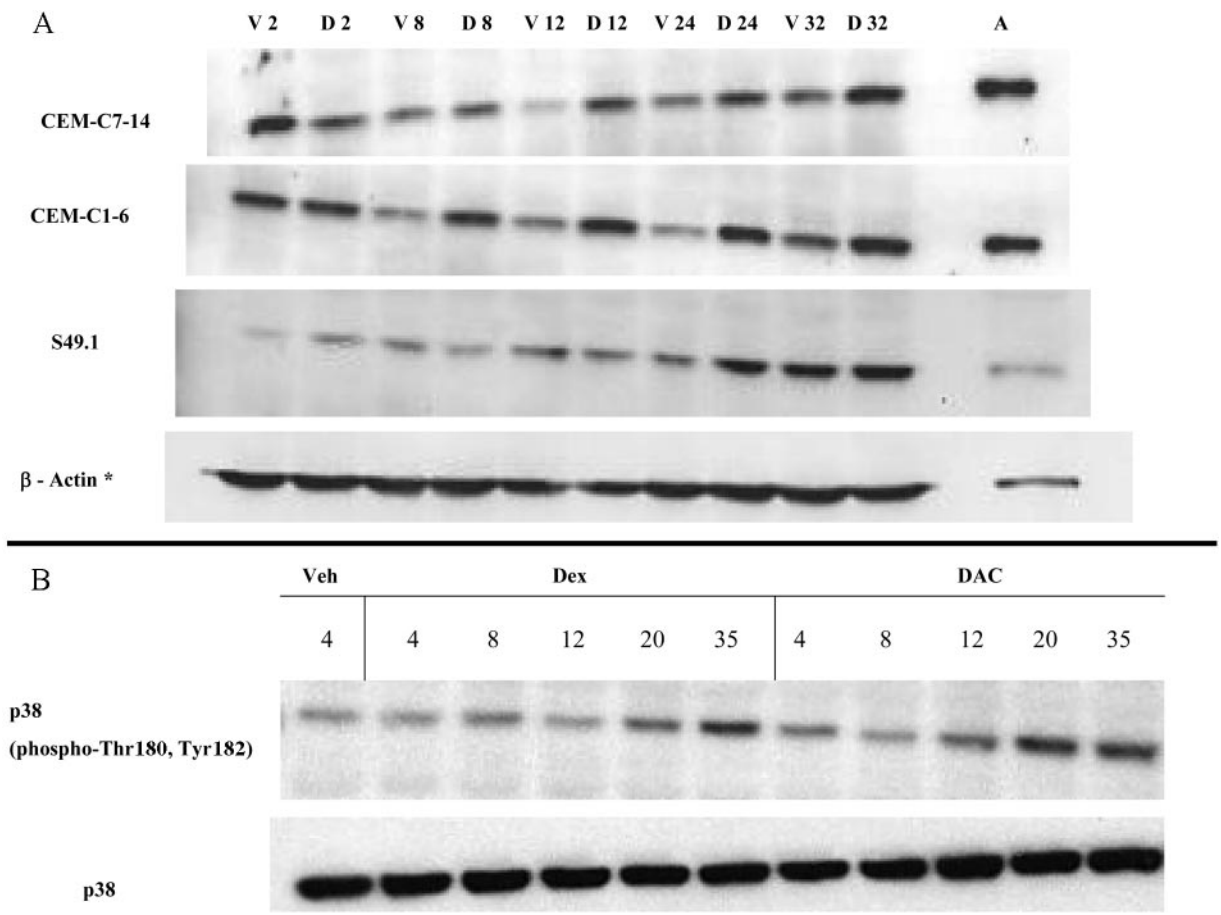

Fig. 6. Time Course of Phosphorylation/Activation of p38 MAPK by GCs

A, Time course for CEM-C7–14, CEM-C1–6, and S49.1 cells plated at a density of 2.0×10^5 viable cells/ml and treated with vehicle (<1% ethanol) (V) or 10^{-6} M Dex (D). Cellular protein was extracted at 2, 8, 12, 24, and 32 h after Dex treatment. Immunoblotting was performed with an antibody for phospho-specific p38 MAPK (threonine180, tyrosine182). A 1-h exposure to the potent JNK/p38 activator anisomycin was used as a positive control (A). As a control for protein loading a second reaction for β-actin was performed on each filter. The reaction from the S49.1 cell filter shown here is representative of all three immunoblots. B, Data from a separate experiment in which CEM-C7–14 cells were plated at a density of 4.0×10^5 viable cells/ml and treated with vehicle (<1% ethanol for Dex, DMSO for DAC), 10^{-6} M Dex, or 10^{-7} M DAC. Cellular protein was extracted at 4, 8, 12, 20, and 35 h after GC treatment. Immunoblotting was performed with antibodies for phospho-specific p38 MAPK (threonine180, tyrosine182, and p38 MAPK protein (p38). A total of three experiments following p38 MAPK phosphorylation were performed, all with similar results.

scription of GRE-driven genes. Plasmids encoding wild-type hGR500 or its gene altered to encode alanine instead of serine at position 211 (S211A) were transfected into the CV-1 cells. To test the consequence of the mutation, a plasmid encoding a promoter that contained a GRE site driving a reporter gene was cotransfected. The results show that the mutant lacking a phosphorylatable amino acid at position 211 was considerably less potent in inducing the reporter gene (Fig. 10). We tested the effect of the S211A mutation on apoptosis driven by hGR500. We have shown previously that in ICR-27 cells (also lacking functional GR), the constitutively active hGR500 causes apoptosis equivalent in extent to that driven by holo-GR (44). The data from two experiments show that ICR-27 cells transfected with the nonphosphorylatable S211A mutant hGR500 showed an average of 60% less cell death than those transfected with nonmutated hGR500 (Fig. 11).

DISCUSSION

We show here that inhibition of the p38 MAPK activity inhibits GC-evoked apoptosis of lymphoid cells from two species, *Homo sapiens* and *Mus musculis*. Data from the use of highly specific chemical inhibitors of p38 α and β MAPK, and of ERK and JNK lead us to this conclusion. Two inhibitors of p38 MAPK were employed, SB203580 and SB202190. These have been tested against at least 24 well-known protein kinases involved in cell signaling paths (47, 48) and shown to be quite specific. Their specificity has been validated

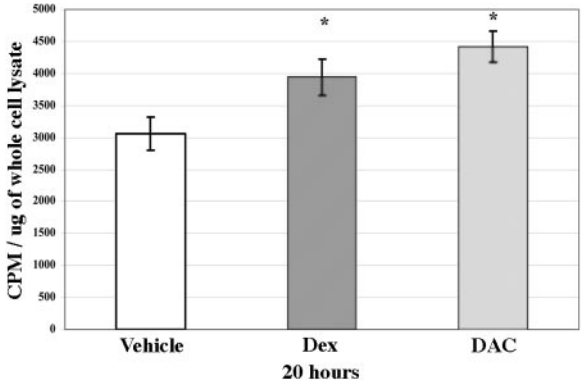

Fig. 7. p38 MAPK Activity Is Increased in Cell Extracts from Cells Treated with GCs

CEM C1–6 cells were grown in nine separate wells to a density of 4.0×10^5 viable cells/ml. Sets of three wells were treated with vehicle (<1% ethanol for Dex, DMSO for DAC), 10^{-6} M Dex, or 10^{-7} M DAC for 20 h. Cellular protein was extracted and p38 MAPK activity was quantitated by measuring its ability to transfer ^{32}P-labeled ATP to a synthetic peptide substrate with subsequent binding to a cellulose filter. The level of radiolabeled peptide was evaluated by scintillation counting. Data are represented as incorporated counts per minute per microgram of whole cell lysate. Statistical significance was evaluated by paired *t* test; *, $P \leq 0.04$, n = 3. Single experiment.

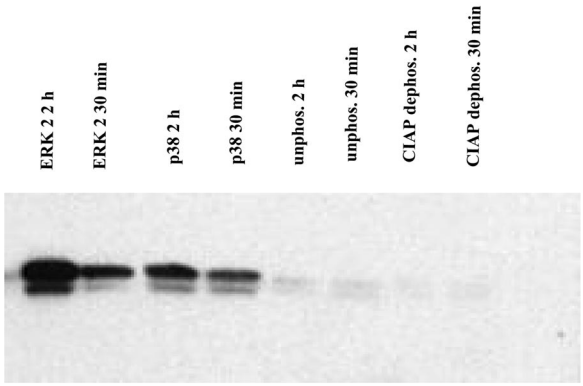

Fig. 8. MAPKs p38 and ERK 2 Phosphorylate S211 of the hGR AF1 *in Vitro*

Purified recombinant hGR AF1 was incubated with assay buffer alone ± active ERK 2, p38, or calf intestine alkaline phosphatase (CIAP). An ATP/Mg^{++} cocktail was added to all samples except the buffer control. Samples were then incubated in a 30 C water bath and harvested after 30 min and 2 h. Proteins were subjected to SDS-PAGE gel electrophoresis and transferred to a PVDF membrane. Immunoblot analysis using an antibody to phospho-specific hGR (S211) indicated phosphorylation in both ERK 2 and p38 treatments. The buffer-only (unphosphorylated) and samples with calf intestine alkaline phosphatase added yielded no positive antibody reactions; n = 2 experiments with p38 MAPK, 1 with ERK 2 because the latter was confirmatory of published results.

further by use of a drug-resistant mutant of p38 (49). The mechanism for this specificity is known. The inhibitors bind the ATP site of p38, and crystal structures show this site to have a special topology among protein kinases, such that the indicated inhibitors are uniquely effective (50–52). To inhibit JNK, we employed a chemically different inhibitor, SP600125, which has an IC_{50} for JNKs 1, 2, and 3 at least two orders of magnitude lower than for 16 other kinases, and one order of magnitude lower for MKK4, a JNK upstream activator (53). We inhibited ERK activity with U0126, which inhibits MEK1/MKK1, the activator of ERK; U0126 has been shown to suppress the activity of the classic MAPK (ERK) cascade in cells (54, 55)

We show that the p38 MAPK blockers significantly reduce the apoptosis due to Dex in four clones derived from the human leukemic cell line CEM and in one clone of mouse lymphoid cells. Thus, in two mammalian species, p38 MAPK is involved in GC-evoked apoptosis. The most marked effect was in ICR-27 cells, a subclone of CEM-C7, derived after chemical mutagenesis and one-step selection for resistance to Dex (34). These cells lack functional GR; when it is replaced, their sensitivity to Dex is restored (35, 44). In these cells, transfected with GR, death due to Dex was prevented by addition of p38 MAPK inhibitor (Fig. 1). To avoid concerns over transient transfections and use of mutagenized cells, and to test the generality of the effect, we also tested two nonmutagenized clones of CEM cells and the S49.1 clone of mouse lymphoid cells, all of which are sensitive to Dex-induced apoptosis. The inhibitors significantly ameliorated the apoptosis in every case, although not as completely as in the GR-transfected ICR-27 cells. It is widely held now that cell paths to death, as for most important biological processes, are multiple and interactive. This is attested to by the fact that the partial protections by cMyc and blocking p38 MAPK are additive (Tables 1 and 2). We ascribe, therefore, the stronger block of apoptosis in ICR-27 cells to the likelihood that the mutagenic treatment that they had received had knocked out other critical paths, leaving the p38 path dominant. Additional studies are planned to test this hypothesis.

Use of other highly specific chemical inhibitors showed that blocking either of the major ERK or JNK pathways enhanced rather than diminished Dex-evoked apoptosis. Thus, the results presented in this paper strongly imply the involvement of p38 MAPK, and not other general MAPK pathways, in GC-dependent lymphoid cell apoptosis. Application of additional, molecular biology-based methods will be required to fully substantiate this conclusion.

Consistent with our primary conclusion is our documentation of p38 MAPK activation following treatment of the cells with two potent, structurally different GCs. This occurred without an increase in p38 protein. When its phosphorylation was used as an index of activation, it took 8 h or more for p38 MAPK to be activated, perhaps a little less with the more active

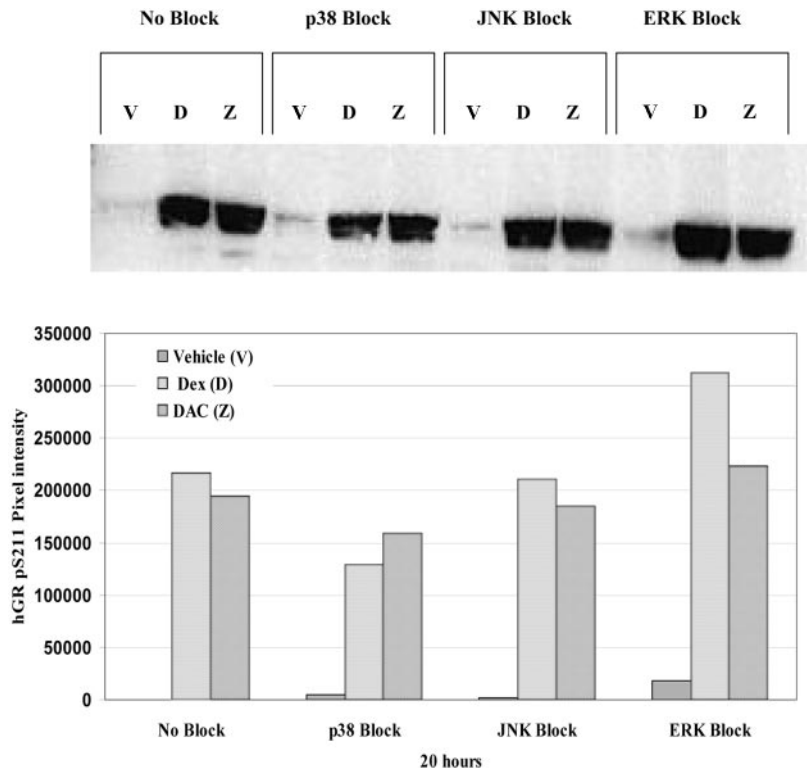

Fig. 9. Inhibition of Cellular p38 MAPK Activity Reduces GC-Dependent Phosphorylation of hGR (S211)

CEM-C7–14 cells were grown to a density of 4.0×10^5 viable cells/ml and treated with vehicle (<1% ethanol/DMSO) (V), 10^{-6} M Dex (D), 10^{-7} M DAC (Z), in the presence or absence of inhibitors for p38 (1.0 μg/ml SB203580), JNK (1.0 μg/ml SP600125), or ERK (1.0 μg/ml U0126) for 20 h. Cellular protein was extracted and immunoblotting was performed with an antibody to phospho-specific hGR (S211). Bands were quantitated densitometrically and the results depicted as a bar graph. n = 1 experiment. Comparable results with Dex and SB203580 were obtained in three additional experiments.

steroid, DAC. We confirmed that p38 was activated by assaying its activity in cell extracts. The slow time course is consistent with prior induction of proteins that ultimately cause the activating phosphorylation of p38. The known immediate upstream activators are MKK3 and MKK6, both specific to p38. In addition, MKK4, whose best-known substrate is JNK, also can phosphorylate p38. Time-course gene array data failed to show induction of MKK4 and MKK6 but suggested a small increase in MKK3 mRNA. We confirmed that this occurred by RT-PCR, Northern blots, and real-time PCR. Induction appeared to be detectable around 8–12 h in clone CEM-C7–14, later in the clone CEM-C1–6. Further work will be required to show whether *mkk*3 induction is rapid enough and sufficient to account fully for the p38 phosphorylation, although *mkk*3 appears to at least contribute.

As to the consequences of p38 MAPK phosphorylation, the many substrates of the kinase offer a wide range of opportunities for investigation. Because of the central role of the GR in the apoptotic process, and of the GR AF1 domain in particular, we focused on this region. So far as we know, it had not been shown previously that p38 phosphorylates hGR S211 *in vivo* or *in vitro*. A recent review lists cyclin-dependent kinase as the only known kinase for the S211 site (56), and earlier work had shown that ERK does not phosphorylate rat GR at the equivalent site (57). The same laboratory has shown that phosphorylation of hGR S211 is increased by Dex treatment of lung cancer and osteosarcoma cell lines, that the phosphorylated S211 hGR is found predominantly in the nucleus, and that the modified hGR has enhanced transcriptional activity (43). We now confirm and extend these findings by showing in lymphoid cells that S211 phosphorylation enhances GRE-dependent transcription. We further show that S211 of AF1 is a specific substrate site for p38 MAPK. This is relevant to GC-driven apoptosis, because the mutation S211A, which prevents phosphorylation at the position, diminishes apoptosis driven by the constitutively active GR lacking the ligand binding domain. The results are diagrammed in Fig. 12 as a testable hypothetical model.

In sum, we here present strong evidence implicating the phosphorylation/activation of the p38 MAPK in the apoptosis evoked by GCs in mouse and human lymphoid cells. Among the MAPKs, p38 is a specific substrate for the kinase kinase MKK3. We show that two different GCs, Dex and DAC, cause a modest but reproducible increase in MKK3 mRNA levels. Neither steroid induced MKK6 or MKK4, the two other MKKs known to phosphorylate p38. Close comparisons of

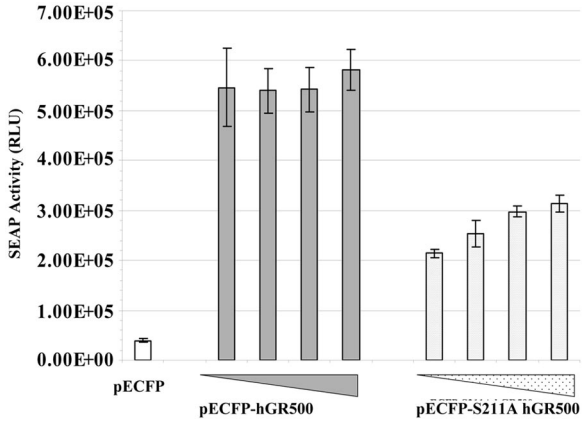

Fig. 10. Mutation of hGR (S211) to a Nonphosphorylatable Amino Acid (Alanine) Reduces GRE-Driven Gene Transcription

SEAP activity induced by pECFP-hGR500 and pECFP-S211A hGR500 was determined by using a pGRE-SEAP reporter vector. CV-1 cells were transfected with 0.13 μg of pGRE-SEAP and 0.13, 0.27, 0.40, and 0.53 μg of pECFP-hGR500 or pECFP-S211A hGR500. Cells were incubated for 24 h, after which the growth medium was tested for SEAP activity using a CSPD chemiluminescent substrate. SEAP activity was determined in duplicates and is represented as relative light units (RLU), with the ranges shown by the *error bars*. Experiment performed twice, comparable results.

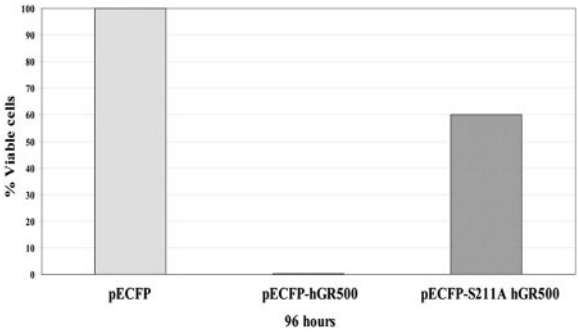

Fig. 11. hGR500-Driven Apoptosis Is Reduced by Mutation of Phosphorylation-Site S211 to Alanine

ICR-27 cells were transfected with pECFP, pECFP-hGR500, or pECFP-S211A hGR500. The remaining viable cells were counted 96 h later using trypan blue exclusion. The reduction in viable cells caused by pECFP-hGR500 was used to define maximum cell kill in each experiment (average of two experiments each in triplicate = 8.5×10^4 cells killed). This is compared with the cell kill by pECFP-S211A hGR500 expressed as percentage of cells killed relative to pECFP-hGR500.

time course and activities of the entire set of kinase kinases will be required to determine whether MKK3 alone is responsible for the p38 activation. We show that a specific site, S211, in the AF1 activation domain of the GR is a substrate for p38. We confirm that phosphorylation of S211 enhances the ability of the GR to stimulate transcription and extend this finding to lymphoid cells. Finally, we show that mutation of S211 to alanine reduces the ability of a constitutively active form of the GR to cause apoptosis. This suggests that the phosphorylation of S211 by the p38 MAPK is at least one mechanism though which the kinase is involved in GR-driven apoptosis.

MATERIALS AND METHODS

Cell Culture

The human CCRF-CEM cell line was isolated from a patient with acute lymphoblastic leukemia. Subclone CEM-C7–14, sensitive to GC-evoked apoptosis, was obtained from the original sensitive CEM-C7 clone (9, 58). Subclone CEM-C1–6 is a GC-sensitive spontaneous revertent from the GC-resistant CEM-C1 clone (9). The GC-resistant clone of ICR-27 cells was derived from the parental CEM-C7 clone after mutagenesis by selection in high-dose Dex (34). ICR-27 cells contain only an inactive mutant hGR allele (59). CEM-C7–14 Myc ER cells, clone 22, have been described (41). S49.1 mouse lymphoma cells and CV-1 African green monkey kidney epithelial cells were obtained from the American Type Culture Collection (ATCC) (Manassas, VA). CEM cells were grown in RPMI 1640 (Cellgro Media Tech, Herndon, VA) (pH 7.4); S49.1 cells were grown in DMEM containing 4.5 g/liter glucose (Invitrogen, Carlsbad, CA) and 1 mM sodium pyruvate (Sigma-Aldrich, St. Louis, MO). CV-1 cells were cultured in MEM with Earle's salt (Invitrogen). All the media were supplemented with heat-inactivated fetal bovine serum (FBS) (Atlanta Biologicals, Norcross, GA), 5% for lymphoid cells and 10% for CV-1 cells. Cells were cultured at 37 C in a humidified atmosphere of 95% air, 5% CO_2, with subculturing at regular intervals to ensure logarithmic growth. Viable cells were determined by their ability to exclude trypan blue dye (Sigma-Aldrich) and were counted by hemacytometer or on a Vi-cell automated cell counter (Beckman Coulter, Miami, FL). In comparisons with various methods for determining apoptosis, we have in many publications shown this to be a reliable way of estimating the ultimate apoptosis in this cellular system. All experiments were initiated in triplicate at 1.0×10^5 viable cells/ml unless otherwise indicated. Cells were treated as appropriate to the experiment with vehicle [ethanol/dimethylsulfoxide (DMSO) $<$1% final concentration], 10^{-6} M Dex, 10^{-7} M DAC (obtained through the kind offices of Dr. J. P. Raynaud, Roussel-UCLAF, Paris, France), 1.0 μg/ml SB203580, 1.0 μg/ml SB202190, 1.0 μg/ml SP600125, or 1.0 μg/ml U0126. All chemicals were from Sigma-Aldrich unless otherwise indicated.

Transient Transfection of ICR-27 Cells by Electroporation

Logarithmically growing ICR-27 cells were collected by centrifugation at 1000 rpm for 5 min at 25 C and washed with 10 ml of sterile 37 C phosphate-buffered isotonic saline, pH 7.4 (PBS). Cells were resuspended to a density of 1.0×10^7 viable cells/ml in serum free 37 C RPMI 1640, and 800 μl aliquots of the suspension were placed into 0.4-cm gap electroporation cuvettes (Bio-Rad, Hercules, CA) containing 15 μg of either pEGFP-C1, pEGFP-hGR, pECFP-C1, pECFP-hGR500, or pECFP-S211A hGR500 (BD CLONTECH, Palo Alto, CA) plasmid DNA. Cuvettes were electroporated using 500 μF and 300 V, using a Gene Pulser II (Bio-Rad). Electroporated cells were then sus-

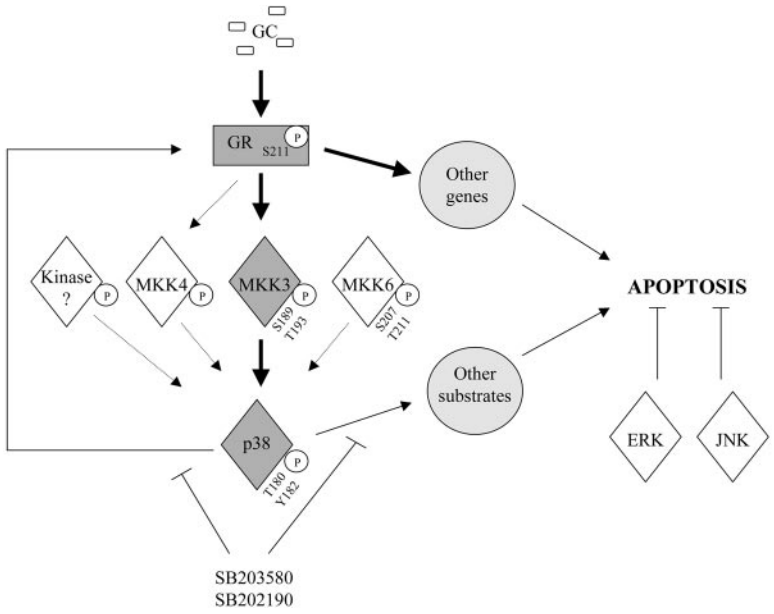

Fig. 12. Interactions of MAPK and GC Pathways in Lymphoid Cell Apoptosis as Supported by Data in this Manuscript

GCs bind and activate the GR, which induces the gene for MKK3 as well as inducing or repressing other genes, which leads to site-specific phosphorylation/activation of p38 MAPK. This kinase phosphorylates many other substrates including the hGR as shown at position S211. This phosphorylation enhances GR:GRE-dependent transcription. Inhibition of p38 MAPK activity reduces GC-driven apoptosis, whereas inhibition of MAPKs ERK or JNK enhance this process.

pended in 10 ml of RPMI 1640 supplemented with 5% FBS and cultured as previously stated. Cells used in the hGR500 *vs.* S211A hGR500 comparison assay were treated with phorbol 12-myristate 13-acetate 50 ng/ml and phytohemagglutinin 1.0 μg/ml final concentration to stimulate transgene expression. Twenty-four hours after electroporation, viable cell numbers were quantified using trypan blue exclusion, diluted to 1.0×10^5 viable cells/ml in RPMI 1640 supplemented with 5% FBS, and treated with vehicle (ethanol/DMSO), 10^{-6} M Dex, 1.0 μg/ml SB203580, 10^{-6} M Dex + 1.0 μg/ml SB203580. Viable cell numbers at various time points after treatment were determined by trypan blue dye exclusion using a Vi-cell automated cell counter.

Apoptotic DNA Lysis and Cell Cycle Evaluation by Propidium Iodide (PI) Staining and Flow Cytometry

Cells were collected by centrifugation, resuspended in 1 ml of 4 C PBS/0.1% sodium azide solution and transferred to 1.5-ml microtubes. In these, the cells were collected at 1000 rpm for 5 min at 4 C. The supernatant liquid was removed and the cells were suspended in low-salt stain (3% polyethylene glycol 8000, 50 μg/ml PI, 4 mM sodium citrate from Mallinckrodt, Hazelwood, MO), plus 0.1% Triton X-100 (Bio-Rad) and 180 U ribonuclease A (Worthington Biochemicals, Lakewood, NJ). The samples were incubated in a 37 C water bath in the dark for 20 min, then an equal volume of high salt stain (3% polyethylene glycol 8000, 50 μg/ml PI, 400 mM sodium citrate, 0.1% Triton X-100) was added. The samples were covered and placed at 4 C for at least 1 h in the dark before analysis. Sample lots were analyzed for DNA content by flow cytometry in the University of Texas Medical Branch core laboratory. *Red*, PI-stained DNA was detected using a 585-nm filter.

Estimation of Specific mRNA Levels

Duplicate cultures of CEM-C7–14 cells grown to a density of 4.0×10^5 viable cells/ml were treated with vehicle (ethanol/DMSO), 10^{-6} M Dex, or 10^{-7} M DAC. Cells were harvested by centrifuging at 1000 rpm at 25 C for 10 min, resuspended in lysis buffer (RNeasy kit, QIAGEN, Valencia, CA), and processed per the instructions of the RNeasy mini-prep kit. The blotting procedure was carried out as previously described (9) with minor modifications. The cDNA for MKK3 was isolated from the plasmid pCMV-Sport6 containing the full-length *mkk3* gene (GenBank ID BC032478, ATCC) and used as a probe in the Northern blot hybridizations. A total of 12 μg of RNA was analyzed for each experimental variable. Audioradiograms were developed on Blue Lite Autorad film (ISC BioExpress, Kaysville, UT) and bands were quantitated by normalization to either 18s or β-actin on an Alpha Innotech Imager (San Leandro, CA). Film linearity was ensured through graphic analysis. Quantitative Real-time RT-PCR was performed using Assays-on-Demand primer mix containing TaqMan MGB probe (FAM dye labeled) to the *mkk3* gene (Applied Biosystems, Foster City, CA). Predeveloped 18s rRNA (VIC dye labeled probe) combined with TaqMan assay reagent (P/N 4319413E) was used as an endogenous control. Separate tube (singleplex) one-step RT-PCR (TaqMan one-step RT-PCR master mix reagent kit; Applied Biosystems) was performed with 80 ng of RNA for both *mkk3* and the endogenous control. One-step RT-PCR was performed using an ABI 7000 sequence detection system (Applied Biosystems) using the following cycling parameters: reverse transcription 48 C for 30 min, AmpliTaq activation 95 C for 10 min, denaturation 95 C for 15 sec, and annealing/extension 60 C for 1 min (40 cycles). Duplicate threshold cycle (C_T) values were analyzed using Microsoft Excel using the comparative $C_T(\Delta\Delta C_T)$ method as described by the manufacturer (Applied Biosystems). The amount of target ($2^{-\Delta\Delta CT}$) was obtained by normalizing to the endogenous reference (18s) relative to a single calibrator (CEM-C7–14 experiment 1, control, 8 h).

Immunochemical Analysis

Cells were grown to a density of 2.0×10^5 or 4.0×10^5 viable cells/ml for phospho and p38 MAPK protein independent of phosphorylation state assays and 4.0×10^5 cells/ml for analysis of hGR S211 phosphorylation *in vivo*. Purified hGR AF1 domain (61) was used for analysis of hGR S211 *in vitro*. For time course experiments, cell cultures were treated with ethanol only or brought to 10^{-6} M Dex by addition of a concentrated stock solution and then recultured for 2–32 h. Cultures were treated with ethanol/DMSO, 10^{-6} M Dex, 10^{-7} M DAC, ± 1.0 μg/ml SB203580, ± 1.0 μg/ml SP600125, or ± 1.0 μg/ml U0126 for 20 h for analysis of hGR S211 phosphorylation state. Cells were pelleted and washed as previously stated. The washed cell pellets were transferred to 1.5-ml centrifuge tubes and lysed on ice using 4 C M-per cell lysis buffer (Pierce, Rockford, IL) supplemented with protease inhibitor cocktail (Sigma-Aldrich), 10 mM sodium fluoride, and 1 mM sodium orthovanadate. Cellular debris was pelleted by centrifugation at 13,000 rpm for 10 min 4 C in a Beckman microfuge. Clarified samples were transferred to fresh cold microfuge tubes, and the protein concentration was estimated using bicinchoninic acid (Pierce). Whole cell lysate (25 μg) was mixed with 5× SDS-PAGE sample buffer supplemented with 2% 2-mercaptoethanol and heated to 100 C for 5 min. Samples were electrophoresed by 10% SDS-PAGE with subsequent transfer to a polyvinylidine difluoride (PVDF) membrane (Bio-Rad; or Amersham Pharmacia Biotech, Piscataway, NJ) using a semidry electroblotter (Bio-Rad). Membranes were washed with Tris-buffered saline (TBS) [140 mM sodium chloride, 20 mM Tris (pH 7.6)] and blocked for 1 h in TBS supplemented with 5% nonfat dry milk. Membranes were washed again and placed in a solution of TBS plus 5% BSA and 0.1% Tween 20 containing either an antibody phospho-(threonine180 and tyrosine182) specific to p38 MAPK (Calbiochem, San Diego, CA), phosphorylation state-independent p38 MAPK (Calbiochem), or hGR phosphoserine 211 (Cell Signaling Technology, Beverly, MA) and incubated for 16 h at 4 C with gentle agitation. Membranes were subsequently washed with TBS supplemented with 0.1% Tween 20. Membranes were probed with a horseradish peroxidase goat/antirabbit secondary antibody for 1 h at 25 C. After again washing, the membranes were saturated with the horseradish peroxide substrate ECL (Amersham Pharmacia Biotech) and exposed to Kodak (Rochester, NY) photographic film for various times to ensure linearity.

Kinase Assay

CEM-C1–6 cells were grown to a density of 4.0×10^5 viable cells/ml and treated in triplicate with vehicle (ethanol/DMSO as appropriate), 10^{-6} M Dex, or 10^{-7} M DAC for 20 h. Cells were harvested and washed as stated. Cell pellets were resuspended in 4 C lysis buffer [20 mM MOPS (pH 7.2), 25 mM β-glycerol phosphate, 5 mM EGTA, 1 mM sodium orthovanadate, 1 mM dithiothreitol, and protease inhibitor cocktail]. Samples were subjected to two cycles of freeze-thaw at −80 C and 30 C. Samples were clarified as described. Protein was quantitated using bicinchoninic acid as previously stated. A kinase assay was then performed as per the instructions of the p38α/SAPK2a assay kit (Upstate, Lake Placid, NY) using 5 μg of whole cell lysate. Data are expressed as incorporated counts per minute per 1 μg protein in whole cell lysate.

Phosphorylation of hGR AF1 S211 *in Vitro*

Recombinant hGR AF1, consisting of amino acids 77 through 262 of the hGR, was expressed and purified as described (60). Protein phosphorylation was carried out by combining 1.0 μg of purified AF1 with 10 μl ATP/Mg^{++} cocktail (500 μM ATP, 75 mM magnesium chloride) (Upstate), 36.5 μl assay dilution buffer [20 mM MOPS (pH 7.2), 25 mM β-glycerophosphate, 5 mM EGTA, 1 mM sodium orthovanadate, 1 mM dithiothreitol], also from Upstate, and 2.5 μl of purified kinases ERK 2, Cdc 2, or casein kinase II (New England Biolabs, Beverly, MA), or active p38 MAPK (Upstate). Two control reactions were as follows: unphosphorylated 1.0 μg AF1 plus 49 μl assay dilution buffer and dephosphorylated 1.0 μg AF1, 1.0 μl calf intestine alkaline phosphatase (New England Biolabs), 5 μl 10× reaction buffer, and 43 μl water. All samples were incubated at 30 C in a water bath with gentle agitation. After 30 min and after 2 h of incubation, 25-μl samples were removed, mixed with 5× sample buffer supplemented with 2% 2-mercaptoethanol and heated to 100 C for 5 min. Samples were then electrophoresed on a 10% SDS-PAGE gel with subsequent transfer to a PVDF membrane (Bio-Rad) using a semidry electroblotter (Bio-Rad). The membrane was probed with an antibody specific to the phosphorylated S211 of the hGR and processed as previously described.

Estimation of Gene Transactivation by hGR500

The recombinant clone hGR500 was fused with the gene for the enhanced cyan fluorescent protein (ECFP) to make the expression plasmid pECFP-hGR500. The analysis plasmid pECFP-S211A hGR500 contained the single mutation S211A in the hGR gene. CV-1 cells were plated in a 24-well plate (500 μl/well) 1 d before transfection. At 95% confluency, cells were cotransfected with 0.13 μg of pGRE-SEAP reporter vector (BD CLONTECH) plus various amounts (0 to 0.5 μg) of pECFP-hGR500 or pECFP-S211A hGR500 using Lipofectamine 2000 (Invitrogen) according to the manufacturer's instructions. The total amount of DNA added was kept fixed at 0.8 μg by addition of pECFP as necessary. The cells were then returned to the 37 C incubator for 24 h, and 50 μl of medium were then collected and tested for presence of secreted placental alkaline phosphatase (SEAP) using the Great EscAPe SEAP Chemiluminescence Detection Kit (BD CLONTECH) according to the protocol provided by the manufacturer.

Acknowledgments

Received December 22, 2004. Accepted March 29, 2005.

Address all correspondence and requests for reprints to: E. Brad Thompson, M.D., Department of Human Biological Chemistry and Genetics, The University of Texas Medical Branch, 301 University Boulevard, Room 5.104, Medical Research Building, Route 1068, Galveston, Texas 77555-1068. E-mail: bthompso@utmb.edu.

This work was supported by grants from the National Institutes of Health, National Cancer Institute [2R01 CA41407 (to E.B.T.)] and National Institute of Diabetes and Digestive and Kidney Diseases [1R01-DK58829 (to R.K.)] and fellowships from the Sealy Center for Structural Biology and the Kempner Foundation (to A.J.C.).

REFERENCES

1. Thompson EB 1999 Mechanisms of T-cell apoptosis by glucocorticoids. Trends Endocrinol Metab 10:353–358
2. Distelhorst CW 2002 Recent insights into the mechanism of glucocortisteroid-induced apoptosis. Cell Death Differ 9:6–19
3. Ashwell JD, Lu FW, Vacchio MS 2004 Glucocorticoids in T cell development and function. Ann Rev Immunol 18: 309–345
4. Thorburn A 2004 Death receptor-induced cell killing. Cell Signal 16:139–144
5. Newmeyer DD, Ferguson-Miller S 2003 Mitochondria: releasing power for life and unleashing the machineries of death. Cell 112:481–490

6. Shaham S 2003 Apoptosis: a process with a (β) NAC for complexity. Cell 114:659–661
7. Aigner T 2002 Apoptosis, necrosis, or whatever: how to find out what really happens? J Pathol 198:1–4
8. Pinkoski MJ, Green DR 2002 Lymphocyte apoptosis: refining the paths to perdition. Curr Opin Hematol 9:43–49
9. Medh RD, Webb MS, Miller AL, Johnson BH, Fofanov Y, Li T, Wood TG, Luxon BA, Thompson EB 2003 Gene expression profile of human lymphoid CEM cells sensitive and resistant to glucocorticoid-evoked apoptosis. Genomics 81:543–555
10. Thompson EB 1998 The many roles of c-Myc in apoptosis. Annu Rev Physiol 60:575–600
11. Obexer P, Certa U, Kofler R, Helmberg A 2001 Expression profiling of glucocorticoid-treated T-ALL cell lines: rapid repression of multiple genes involved in RNA-, protein- and nucleotide synthesis. Oncogene 20: 4324–4336
12. Wang Z, Malone MH, He H, McColl KS, Distelhorst CW 2003 Microarray analysis uncovers the induction of the proapoptotic BH3-only protein Bim in multiple models of glucocorticoid-induced apoptosis. J Biol Chem 278: 23861–23867
13. Gruol DJ, Rajah FM, Bourgeois S 1989 Cyclic AMP-dependent protein kinase modulation of the glucocorticoid-induced cytolytic response in murine T-lymphoma cells. Mol Endocrinol 3:2119–2127
14. Medh RD, Saeed MF, Johnson BH, Thompson EB 1998 Resistance of human leukemic CEM-C1 cells is overcome by synergism between glucocorticoid and protein kinase A pathways: correlation with c-Myc suppression. Cancer Res 58:3684–3693
15. Ogawa R, Streiff MB, Bugayenko, A, Kato GJ 2002 Inhibition of PDE4 phosphodiesterase activity induces growth suppression, apoptosis, glucocorticoid sensitivity, p53, and p21 (WAF1/CIP1) proteins in human acute lymphoblastic leukemia cells. Blood 99:3390–3397
16. Tanaka H, Makino Y, Okamoto K, Iida T, Yan K, Yoshikawa N 1999 Redox regulation of the glucocorticoid receptor. Antioxid Redox Signal 1:403–423
17. Werlen G, Jacinto E, Xia Y, Karin M 1998 Calcineurin preferentially synergizes with PKC-θ to activate JNK and IL-2 promoter in T lymphocytes. EMBO J 17:3101–3111
18. Gutcher I, Webb PR, Anderson NG 2003 The isoform-specific regulation of apoptosis by protein kinase C. Cell Mol Life Sci 60:1061–1070
19. Jiffar T, Kurinna S, Suck G, Carlson-Bremer D, Ricciardi MR, Konopleva M, Andreeff M, Ruvolo PP 2004 PKCα mediates chemoresistance in acute lymphoblastic leukemia through effects on Bcl2 phosphorylation. Leukemia 18:505–512
20. Caron-Leslie LA, Cidlowski JA 1991 Similar actions of glucocorticoids and calcium on the regulation of apoptosis in S49 cells. Mol Endocrinol 5:1169–1179
21. Pongracz J, Parnell S, Anderson G, Jaffrezou JP, Jenkinson E 2003 Con A activates an Akt/PKB dependent survival mechanism to modulate TCR induced cell death in double positive thymocytes. Mol Immunol 39: 1013–1023
22. Rogatsky I, Logan SK, Garabedian MJ 1998 Antagonism of glucocorticoid receptor transcriptional activation by the c-Jun N-terminal kinase. Proc Natl Acad Sci USA 95:2050–2055
23. Clark AR, Lasa M 2003 Crosstalk between glucocorticoids and mitogen-activated protein kinase signaling pathways. Curr Opin Pharm 3:404–411
24. Szatmary Z, Garabedian MJ, Vilcek J 2004 Inhibition of glucocorticoid receptor-mediated transcriptional activation by p38 mitogen-activated protein (MAP) kinase. J Biol Chem 279:43708–43715
25. Tsitoura DC, Rothman PB 2004 Enhancement of MEK/ERK signaling promotes glucocorticoid resistance in $CD4^+$ T cells. J Clin Invest 113:619–627
26. Huang S, Jiang Y, Li Z, Nishida E, Mathias P, Lin S, Ulevitch RJ, Nemerow GR, Han J 1997 Apoptosis signaling pathway in T cells is composed of ICE/Ced-3 Family proteases and MAP kinase kinase 6b. Immunity 6:739–749
27. Jarpe MB, Widmann C, Knall C, Schlesinger TK, Gibson S, Yujiri T, Fanger GR, Gelfand EW, Johnson GL 1998 Anti-apoptotic versus pro-apoptotic signal transduction: checkpoints and stop signs along the road to death. Oncogene 17:1475–1482
28. Rolli-Derkinderen M, Gaestel M 2000 p38/SAPK2-dependent gene expression in Jurkat T cells. J Biol Chem 381:193–198
29. Jamieson CA, Yamamoto KR 2000 Crosstalk pathway for inhibition of glucocorticoid-induced apoptosis by T cell receptor signaling. Proc Natl Acad Sci USA 97: 7319–7324
30. Tanaka N, Kamanaka M, Enslen H, Dong C, Wysk M, Davis RJ, Flavell RA 2002 Differential involvement of p38 mitogen-activated protein kinase kinases MKK3 and MKK6 in T-cell apoptosis. EMBO Rep 3:785–791
31. Platanias LC 2003 Map kinase signaling pathways and hematologic malignancies. Blood 101:4667–4679
32. Hsu SC, Wu CC, Han J, Lai MZ 2003 Involvement of p38 mitogen-activated protein kinase in different stages of thymocyte development. Blood 101:970–976
33. Olson JM, Hallahan AR 2004 p38 MAP kinase: a convergence point in cancer therapy. Trends Mol Med 10: 125–129
34. Harmon JM, Thompson EB 1981 Isolation and characterization of dexamethasone-resistant mutants from human lymphoid cell line CEM-C7. Mol Cell Biol 1:512–521
35. Harbour DV, Chambon P, Thompson EB 1990 Steroid mediated lysis of lymphoblasts requires the DNA binding region of the steroid hormone receptor. J Steroid Biochem 35:1–9
36. Baxter JD, Harris AW, Tomkins GM, Cohn M 1971 Glucocorticoid receptors in lymphoma cells in culture: relationship to glucocorticoid killing activity. Science 171: 189–191
37. Johnson BH, Ayala-Torres S, Chan LNL, El-Naghy M, Thompson EB 1997 Glucocorticoid/oxysterol-induced DNA lysis in human leukemic cells. J Steroid Biochem Mol Biol 61:35–45
38. Yuh YS, Thompson EB 1989 Glucocorticoid effect on oncogene/growth gene expression in human T-lymphoblastic leukemic cell line CCRF-CEM: specific c-myc mRNA suppression by dexamethasone. J Biol Chem 264:10904–10910
39. Thulasi R, Harbour DV, Thompson EB 1993 Suppression of c-myc is a critical step in glucocorticoid-induced human leukemic cell lysis. J Biol Chem 268:18306–18312
40. Zhou F, Medh RD, Thompson EB 2000 Glucocorticoid mediated transcriptional repression of c-myc in apoptotic human leukemic CEM cells. J Steroid Biochem Mol Biol 73:195–202
41. Medh RD, Wang A, Zhou F, Thompson EB 2001 Constitutive expression of ectopic c-myc delays glucocorticoid-evoked apoptosis of human leukemic CEM-C7 cells. Oncogene 20:4629–4639
42. Wang Z, Frederick J, Garabedian MJ 2002 Deciphering the phosphorylation "code" of the glucocorticoid receptor in vivo. J Biol Chem 277:26573–26580
43. Godowski PJ, Rusconi S, Miesfeld R, Yamamoto KR 1987 Glucocorticoid receptor mutants that are constitutive activators of transcriptional enhancement. Nature 325:365–368
44. Nazareth LV, Harbour DV, Thompson EB 1991 Mapping the human glucocorticoid receptor for leukemic cell death. J Biol Chem 266:12976–12980

45. Chen H, Srinivasan G, Thompson EB 1997 Protein: protein interactions are implied in glucocorticoid receptor mutant 465* mediated cell death. J Biol Chem 272: 25873–25880
46. Kumar R, Baskakov IV, Srinivasan G, Bolen DW, Lee JC, Thompson EB 1999 Interdomain signaling in a two-domain fragment of the human glucocorticoid receptor. J Biol Chem 274:24737–24741
47. Cuenda A, Rouse J, Doza YN, Meier R, Cohen P, Gallagher TF, Young PR, Lee JC 1995 SB203580 is a specific inhibitor of a MAP kinase homologue which is stimulated by cellular stresses and interleukin-1. FEBS Lett 364:229–233
48. Davies SP, Reddy H, Caivano M, Cohen P 2000 Specificity and mechanism of action of some commonly used protein kinase inhibitors. Biochem J 351:95–105
49. Eyers PA, van den IJssel P, Quinlan RA, Goedert M, Cohen P 1999 Use of a drug-resistant mutant of stress-activated protein kinase 2a/p38 to validate the in vivo specificity of SB203580. FEBS Lett 451:191–196
50. Tong L, Pav S, White DA, Rogers S, Crane KM, Cywin CL, Brown ML, Pargellis CA 1997 A highly specific inhibitor of human p38 MAP kinase binds in the ATP pocket. Nat Struct Biol 4:311–316
51. Wilson KP, McCaffrey PG, Hsiao K. Pazhanisamy S, Galullo V, Bemis GW, Fitzgibbon MJ, Caron PR, Murcko MA, Su MSS 1997 The structural basis for the specificity of pyridinylimidazole inhibitors of p38 MAP kinase. Chem Biol 4:423–431
52. Young PR, McLaughlin MM, Kumar S, Kassis S, Doyle, ML, McNulty D, Gallagher TF, Fisher S, McDonnell PC, Carr SA, Huddleston MJ, Seibel G, Porter TG, Livi GP, Adams JL, Lee JC 1997 Pyridinyl imidazole inhibitors of p38 mitogen-activated protein kinase bind in the ATP site. J Biol Chem 272:12115–12121
53. Bennett BL, Sasaki DT, Murray BW, O'Leary EC, Sakata ST, Xu W, Leisten JC, Motiwala A, Pierce S, Satoh Y, Bhagwat SS, Manning AM, Anderson DW 2001 SP600125, an anthrapyrazolone inhibitor of Jun N-terminal kinase. Proc Natl Acad Sci USA 98:13681–13686
54. Favata MF, Horiuchi KY, Manos EJ, Daulerio AJ, Stradley DA, Feeser WS, Van Dyk DE, Pitts WJ, Earl RA, Hobbs F, Copeland RA, Magolda RL, Scherle PA, Trzaskos JM 1998 Identification of a novel inhibitor of mitogen-activated protein kinase kinase. J Biol Chem 273: 18623–18632
55. DeSilva DR, Jones EA, Favata MF, Jaffee BD, Magolda RL, Trzaskos JM, Scherle PA 1999 Inhibition of mitogen-activated protein kinase blocks T cell proliferation but does not induce or prevent anergy. J Immunol 160: 4175–4181
56. Ismaili N, Garabedian MJ 2004 Modulation of glucocorticoid receptor function via phosphorylation. Ann NY Acad Sci 1024:86–101
57. Krstic MD, Rogatsky I, Yamamoto KR, Garabedian MJ 1997 Mitogen-activated and cyclin-dependent protein kinases selectively and differentially modulate transcriptional enhancement by the glucocorticoid receptor. Mol Cell Biol 17:3947–3954
58. Norman MR, Thompson EB 1977 Characterization of a glucocorticoid-sensitive human lymphoid cell line. Cancer Res 37:3785–3791
59. Powers JH, Hillmann AG, Tang DC, Harmon JM 1993 Cloning and expression of mutant glucocorticoid receptors from glucocorticoid-sensitive and -resistant human leukemic cells. Cancer Res 53:4059–4065
60. Kumar R, Lee JC, Bolen DW, Thompson EB 2001 The conformation of the glucocorticoid receptor AF1/tau1 domain induced by osmolyte binds co-regulatory proteins. J Biol Chem 276:18146–18152

Molecular Endocrinology **is published monthly by The Endocrine Society (http://www.endo-society.org), the foremost professional society serving the endocrine community.**